

# High-frequency hopping conductivity in the quantum Hall effect regime: Acoustical studies

I. L. Drichko<sup>a</sup>, A. M. Diakonov<sup>a</sup>, I. Yu. Smirnov<sup>a</sup>, Yu. M. Galperin<sup>a,b</sup>, and A. I. Toropov<sup>c</sup>

<sup>a</sup>*A. F. Ioffe Physico-Technical Institute of Russian Academy of Sciences, Polytechnicheskaya 26, 194021, St.Petersburg, Russia;*

<sup>b</sup>*Centre for Advanced Studies, Drammensveien 78, 0271 Oslo, Norway, and Department of Physics, University of Oslo, P. O. Box 1048 Blindern, 0316 Oslo, Norway;*

<sup>c</sup>*Semiconductors Physics Institute of Siberian Division of Russian Academy of Sciences, Ak. Lavrentieva 13, 630090, Novosibirsk, Russia*

(February 1, 2008)

The high-frequency conductivity of Si  $\delta$ -doped GaAs/AlGaAs heterostructures is studied in the integer quantum Hall effect (QHE) regime, using acoustic methods. Both the real and the imaginary parts of the complex conductivity are determined from the experimentally observed magnetic field and temperature dependences of the velocity and the attenuation of a surface acoustic wave. It is demonstrated that in structures with carrier density  $(1.3 - 2.8) \times 10^{11} \text{ cm}^{-2}$  and mobility  $(1 - 2) \times 10^5 \text{ cm}^2/\text{V}\cdot\text{s}$  the mechanism of low-temperature conductance near the QHE plateau centers is hopping. It is also shown that at magnetic fields corresponding to filling factors 2 and 4, the doped Si  $\delta$ -layer efficiently shunts the conductance in the two-dimensional electron gas (2DEG) channel. A method to separate the two contributions to the real part of the conductivity is developed, and the localization length in the 2DEG channel is estimated.

PACS numbers: 72.50.+b; 73.40.Kp

## I. INTRODUCTION

It is well known from numerous low-temperature resistivity measurements that the electronic states of a two-dimensional electron gas (2DEG) whose energies are located between two adjacent Landau levels in a perpendicular magnetic field are localized. Consequently, the conductance is determined by electron hopping between the localized states. The hopping mechanism is temperature-dependent. At temperatures 1-4 K, the conductance  $\sigma$  is usually determined by nearest-neighbor hopping. In this case its temperature dependence is mainly exponential,  $\sigma_{xx}(T) \propto \exp(-E/kT)$  where  $E$  is the temperature-independent activation energy, see e. g. Refs. 1-3 and references therein. (We assume that the 2DEG is located in the  $x - y$  plane, the magnetic field is parallel to the  $z$ -axis, and the electric field is along the  $x$ -axis.) At lower temperatures,  $T \lesssim 1$  K, the electron hopping distance appears to be greater than the typical distance between nearest neighbors: at such low temperatures it becomes difficult to find a neighbor whose energy is close to the initial one within the accuracy  $kT$ . In this so-called *variable-range-hopping* regime the conductivity  $\sigma_{xx}$  is also exponentially small,<sup>2,4-6</sup> but with an effective activation energy  $E$  which is temperature-dependent.

To clarify the nature of the localized states, we study in this paper the two-dimensional *high-frequency* (hf) conductance of a 2DEG,  $\sigma_{xx}(\omega)$ , by measuring the velocity and the attenuation of surface acoustic waves (SAW) propagating along the  $x$ -direction nearby the electron layer. Acoustic methods are particularly promising for our task since  $|\sigma_{xx}(\omega)|$  in the hopping regime may be of the same order of magnitude as the SAW velocity  $V$ .

Because the screening of the electric fields produced by the SAW is determined by the ratio  $\sigma_{xx}/V$ , the acoustic properties are sensitive to the variations in  $\sigma_{xx}$ . Furthermore, the attenuation and the velocity of the SAW depend on the *complex* conductance,

$$\sigma_{xx}(\omega) \equiv \sigma_1(\omega) - i\sigma_2(\omega),$$

and hence both the active,  $\sigma_1$ , and the reactive,  $\sigma_2$ , components can be detected. The active component can be then compared to the static conductivity,  $\sigma_{dc}$ . A pronounced difference will clearly indicate that the electron states are localized. We compare the experimental results for  $\sigma_1(\omega)$  and  $\sigma_2(\omega)$  with existing models for the dielectric response of localized states and extract relevant parameters of the latter.

The paper is organized as follows. In Sec. II the experimental setup is presented. Experimental results and their discussion are given in Sec. III. They are summarized in Sec. IV. Details of the derivation of the expressions we use are presented in the Appendix.

## II. THE EXPERIMENTAL SETUP

A sketch of the experimental setup is shown in Fig. 1. A SAW propagating along the surface of a piezoelectric crystal is accompanied by a wave of hf electric field. This electric field penetrates into a 2DEG located in a semiconductor heterostructure mounted on the surface. The field produces electrical currents which, in turn, cause Joule losses. As a result, there are electron-induced contributions both to the SAW attenuation and to its velocity. These effects are governed by the complex frequencyy

dependent conductivity,  $\sigma_{xx}(\omega)$ , which oscillates as a function of the external magnetic field. Hence, specific oscillations will appear both in the SAW attenuation and its velocity. Under reasonable assumptions, the experimental results allow one to determine  $\sigma_{xx}(\omega)$  as function of the magnetic field and to analyze its properties.

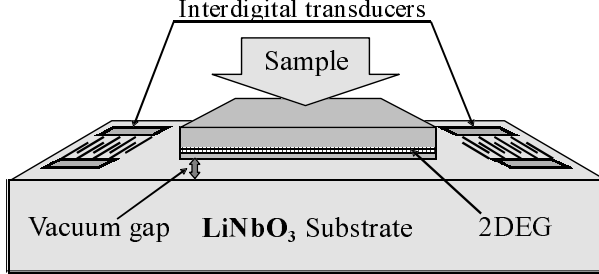


FIG. 1. The experimental setup

In the present work, the attenuation coefficient  $\Gamma$  and the relative velocity change,  $\Delta V/V$ , are measured as functions of perpendicular magnetic field up to 7 T in the temperature interval 1.5–4.2 K. The Si  $\delta$ -doped GaAs/AlGaAs heterostructure samples with sheet densities  $n = (1.3 - 2.7) \times 10^{11} \text{ cm}^{-2}$  and mobilities  $\mu = (1 - 2) \times 10^5 \text{ cm}^2/\text{V}\cdot\text{s}$  at  $T=4.2$  K were grown by molecular-beam epitaxy, their structures being shown in Fig. 2.

### III. EXPERIMENTAL RESULTS AND THEIR DISCUSSION

The expressions relating  $\Gamma$  and  $\Delta V/V$  to the complex conductance,  $\sigma_1 - i\sigma_2$ , can be extracted from Refs. 7 and 8. They read

$$\Gamma (\text{dB/cm}) = 4.34 AK^2 k \gamma, \quad (1)$$

$$\Delta V/V = (AK^2/2) (\delta v/v). \quad (2)$$

Here  $k = \omega/V$  is the SAW wave vector,  $K^2$  is the piezoelectric coupling constant of the substrate (Y-cut LiNbO<sub>3</sub>), and

$$A = 8b(k)(\varepsilon_1 + \varepsilon_0)\varepsilon_0^2\varepsilon_s e^{-2k(a+d)}, \quad (3)$$

$$b(k) = (b_1(k)[b_2(k) - b_3(k)])^{-1}, \quad (4)$$

$$b_1(k) = (\varepsilon_1 + \varepsilon_0)(\varepsilon_s + \varepsilon_0) - (\varepsilon_1 - \varepsilon_0)(\varepsilon_s - \varepsilon_0)e^{(-2ka)}, \quad (5)$$

$$b_2(k) = (\varepsilon_1 + \varepsilon_0)(\varepsilon_s + \varepsilon_0) + (\varepsilon_1 + \varepsilon_0)(\varepsilon_s - \varepsilon_0)e^{(-2kd)}, \quad (6)$$

$$b_3(k) = (\varepsilon_1 - \varepsilon_0)(\varepsilon_s - \varepsilon_0)e^{(-2ka)} + (\varepsilon_1 - \varepsilon_0) \times (\varepsilon_s + \varepsilon_0)e^{[-2k(a+d)]}. \quad (7)$$

In these equations,  $\varepsilon_1=50$ ,  $\varepsilon_0=1$  and  $\varepsilon_s=12$  are the dielectric constants of LiNbO<sub>3</sub>, of the vacuum and of the semiconductor, respectively.  $a$  is the finite vacuum clearance between the sample surface and the LiNbO<sub>3</sub> surface,

which can be determined from acoustical measurements.<sup>9</sup>  $d$  denotes the finite distance between the sample surface and the 2DEG layer. The parameters of our experimental set are  $a = 0.5 \mu\text{m}$ ,  $d = 0.59 \mu\text{m}$  for the first sample, and  $0.09 \mu\text{m}$  for the second one. The reduced attenuation  $\gamma$  and velocity variation  $\Delta V/V$  are given by the expressions

$$\gamma = \frac{\Sigma_1}{\Sigma_1^2 + (1 + \Sigma_2)^2}, \quad \Delta V/V = \frac{1 + \Sigma_2}{\Sigma_1^2 + (1 + \Sigma_2)^2}; \quad (8)$$

$$\Sigma_i = (4\pi\sigma_i/\varepsilon_s V) t(k), \quad t(k) = [b_2(k) - b_3(k)]/2b_1(k).$$

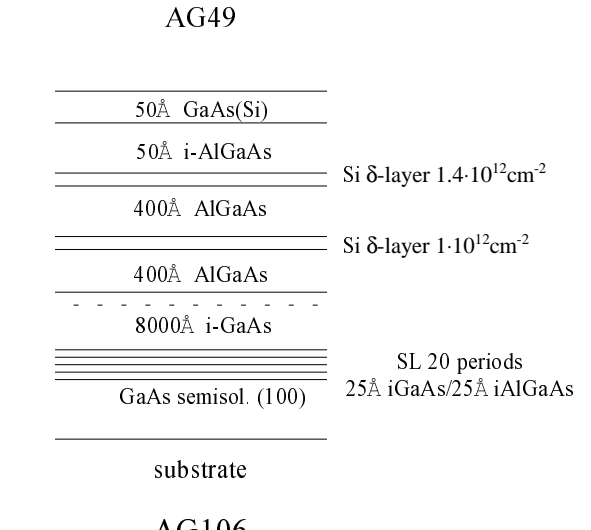
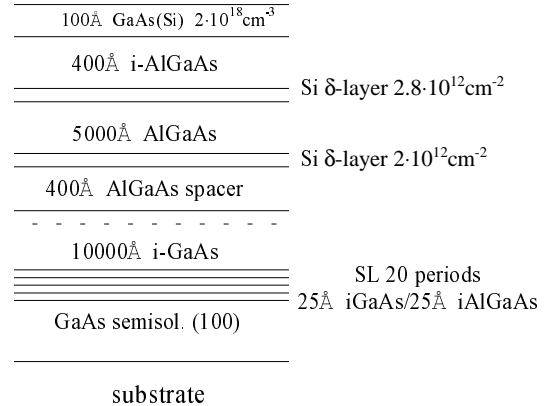


FIG. 2. The structures of the samples AG49 and AG106

The experimental magnetic field dependence of  $\gamma$  and  $\Delta V/V$  for the sample with carrier density  $n = 2.7 \times 10^{11} \text{ cm}^{-2}$  and mobility  $\mu = 2 \times 10^5 \text{ cm}^2/\text{V}\cdot\text{s}$  are shown in Fig. 3. Similar results have been found previously in GaAs/AlGaAs heterostructures.<sup>10</sup>

The real and the imaginary parts of the complex conductance are derived from  $\Gamma$  and  $\Delta V/V$ , using Eqs. (1) and (2). The results obtained for  $T = 1.5$  K and acoustic frequency 30 MHz are shown in Fig. 4.

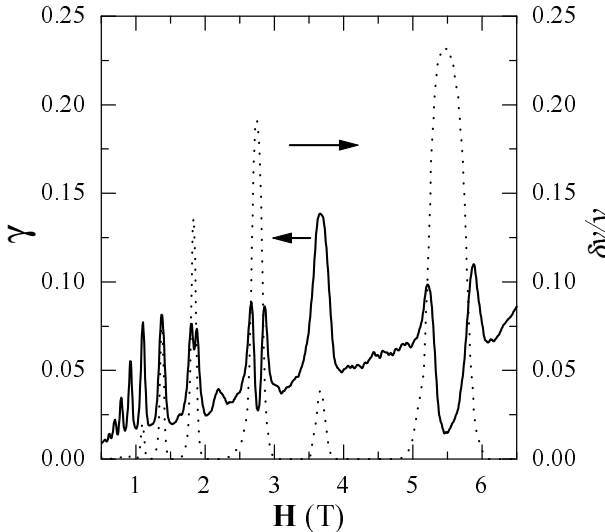


FIG. 3. The experimental dependences of  $\Gamma$  and  $\Delta V/V$  on the perpendicular magnetic field  $H$ .  $T = 1.5$  K,  $f = 30$  MHz.

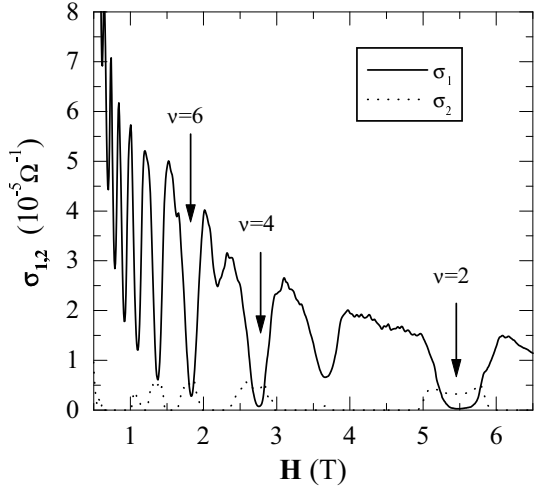


FIG. 4. The experimental dependences of  $\sigma_1$  and  $\sigma_2$  on the perpendicular magnetic field  $H$ .  $T = 1.5$  K,  $f = 30$  MHz.

As can be seen,  $\sigma_2$  practically vanishes near half-integer filling factors, i. e. when the Fermi level is close to any Landau level. In such regions  $\sigma_1(\omega)$ , as has been shown in Ref. 11, appears to be close to the static conductivity,  $\sigma_{dc}$ . These facts indicate that the electron states are indeed *extended*. With a further increase of the magnetic field the Fermi level leaves the Landau band, a metal-dielectric transition takes place, and the electrons become localized in the randomly fluctuating potential of the charged impurities.

As the Fermi level departs from the Landau level center,  $\sigma_1(\omega)$  becomes clearly larger than  $\sigma_{dc}$ , see Fig. 5. Such a behavior can be qualitatively interpreted<sup>11</sup> as absorption by large clusters (“lakes”) disconnected from each other. Inside each cluster the absorption is determined by the value of  $\sigma_{dc}$ . Since the area occupied by the clusters is less than the area occupied by the infinite

cluster at the mobility edge, the effective  $\sigma_1(\omega)$  is less than  $\sigma_{dc}$  at half-integer  $\nu$ . At the same time,  $\sigma_1(\omega)$  is greater than  $\sigma_{dc}$  in the same magnetic field because there is no infinite conducting cluster at the Fermi level. The imaginary part,  $\sigma_2(\omega)$  increases as the Fermi level departs from the Landau level’s center.

At magnetic fields corresponding to small integer filling factors, when the Fermi level finds itself in-between the adjacent Landau levels, where  $\sigma_{dc} \approx 0$ ,  $\sigma_2(\omega)$  becomes about an order of magnitude larger than  $\sigma_1$ , see Fig. 6.

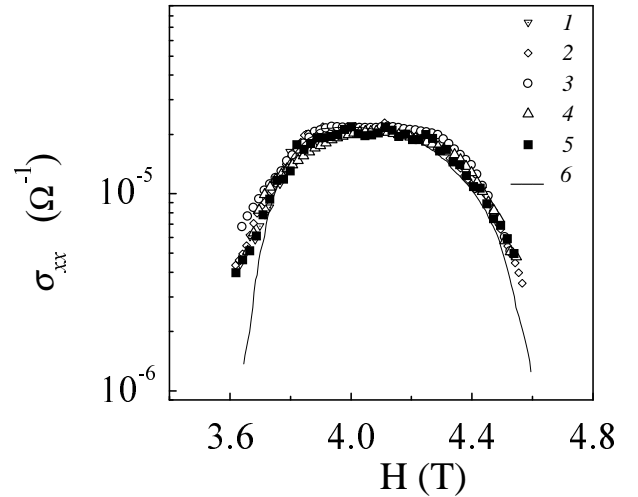


FIG. 5.  $\sigma_{dc}$  (solid line) and  $\sigma_1(\omega)$  versus  $H$  in the region close to the fourth Landau level center. The symbols correspond to frequencies  $f$  (MHz) and vacuum gap widths  $a$  ( $\mu\text{m}$ ): 1 - 213 and 0.3, 2 - 30 and 0.5, 3 - 150 and 0.3, 4 - 30 and 0.4, 5 - 90 and 1.2.  $T = 4.2$  K, the electron density is  $n = 7 \times 10^{11} \text{ cm}^{-2}$ .

Figure 7 depicts the temperature dependences of  $\sigma_1(\omega)$  at  $f=30$  MHz in magnetic fields corresponding to the mid-points of the Hall plateaus. One can see a crossover from a smooth temperature dependence at a strong magnetic field (5.5 T), to a rather steep increase with temperature at weaker fields. Such behavior is compatible with the idea that the conductivity consists of two contributions. The first one is due to the extended states near the adjacent upper Landau level, while the second is coming from the localized states at the Fermi level.<sup>12</sup> The relative occupation of the extended states increases with increasing temperature because of thermally activated processes. Obviously, this effect is dominant at small magnetic fields.

We now turn to the region of low temperatures and filling factors close to 2, where hopping between the localized states gives the main contribution to dielectric response. To analyze the experimental results we adopt the so-called *two-site approximation*, according to which an electron hops between states with close energies localized at two different impurity centers. These states form *pair complexes* which do not overlap. Therefore, they do not contribute to the static conductivity but are

important for the ac response.

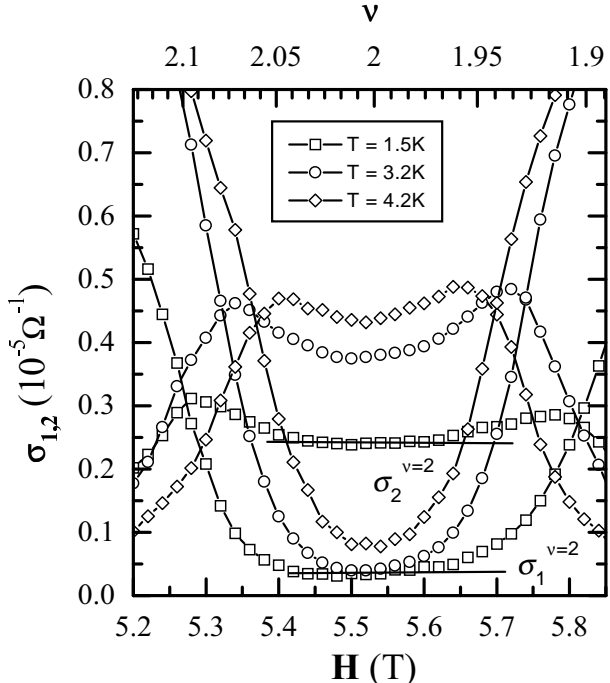


FIG. 6. Magnetic field dependences of  $\sigma_1(\omega)$  and  $\sigma_2(\omega)$  near the filling factor  $\nu = 2$  at  $T = 1.5 - 4.2$  K,  $f = \omega/2\pi = 30$  MHz for the sample with  $n = 2.7 \times 10^{11}$   $\text{cm}^{-2}$  (AG49).

Being a very simple, the two-site model has been extensively studied, see for a review Refs. 13–15 and references therein. In the following we will use the 2D version of the theory.<sup>13</sup> Some details of the discussion depend on the assumptions regarding both the density of localized states and the relaxation mechanisms of their population. We therefore re-derive the theoretical results in Appendix A.

As is well known<sup>14</sup>, there are two specific contributions to the high-frequency absorption. The first contribution, the so-called *resonant*, is due to direct absorption of microwave quanta accompanied by inter-level transitions. The second one, the so-called *relaxational*, or *phonon-assisted*, is due to phonon-assisted transitions which lead to a lag of the levels populations with respect to the microwave-induced variation in the inter-level spacing. The relative importance of the two mechanisms depends on the frequency  $\omega$ , the temperature  $T$ , as well as on sample parameters. The most important of them is the relaxation rate  $\gamma_0(T)$  of *symmetric* pairs with inter-level spacing  $E = kT$ . At  $\omega \lesssim \sqrt{kT\gamma_0/\hbar}$  the relaxation contribution to  $\sigma_1(\omega)$  dominates, and only this one will be taken into account. Following the derivation given in Appendix A we obtain

$$\sigma_1 = \frac{\pi^2}{2} \frac{g^2 \xi^3 \omega e^4}{\varepsilon_s} (\mathcal{L}_T + \mathcal{L}_\omega/2)^2. \quad (9)$$

Here  $g$  is the (constant) single-electron density of states at the Fermi level,  $\xi$  is the localization length of the elec-

tron state,  $\mathcal{L}_T = \ln J/kT$ ,  $J$  is a typical value of the energy overlap integral which is of the order of the Bohr energy, while  $\mathcal{L}_\omega = \ln(\gamma_0/\omega)$ . Eq. (9) is valid provided that the logarithmic factors are large. Note that the product  $r_\omega = \xi(\mathcal{L}_T + \mathcal{L}_\omega/2)$  is the distance between the sites forming a hopping pair. Note also that (9) is similar to the result obtained in Ref. 13, but differs from it by some logarithmic factors and a numerical factor of 1/4.

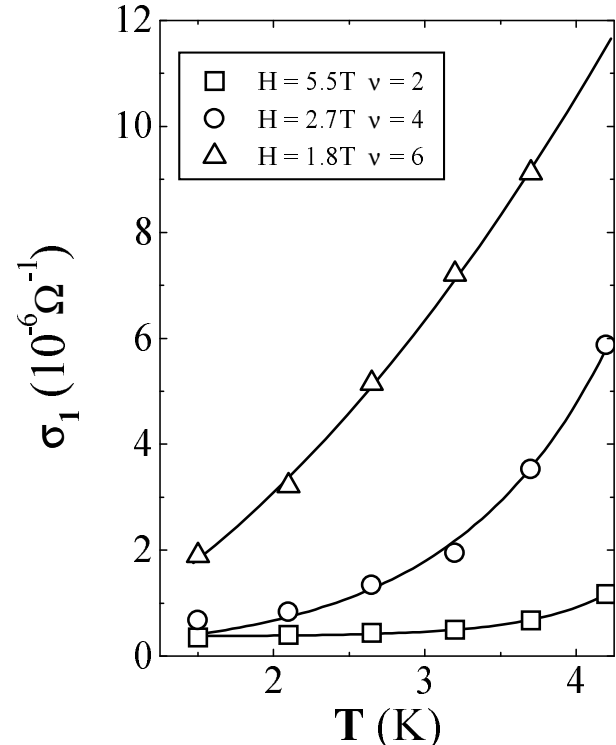


FIG. 7. Temperature dependences of  $\sigma_1(\omega)$  at  $f = 30$  MHz in magnetic fields corresponding to integer filling factors.

The analysis of  $\sigma_2(\omega)$  is a bit more complicated because virtual zero-phonon transitions give a comparable contribution. The analysis presented in Appendix A leads to the following expression for the ratio  $\sigma_2(\omega)/\sigma_1(\omega)$ ,

$$\frac{\sigma_2}{\sigma_1} = \frac{2\mathcal{L}_\omega(\mathcal{L}_T^2 + \mathcal{L}_T\mathcal{L}_\omega/2 + \mathcal{L}_\omega^2/12) + 4c\mathcal{L}_T^2\mathcal{L}_c}{\pi(\mathcal{L}_T^2 + \mathcal{L}_T\mathcal{L}_\omega + \mathcal{L}_\omega^2/4)}. \quad (10)$$

Here  $\mathcal{L}_c = \ln(\hbar\omega_c/kT)$ ,  $\omega_c$  is the cyclotron frequency, and  $c \gtrsim 1$  is a numerical factor depending on the density of states in the region between the Landau levels, see Appendix A. Using the estimate for  $\gamma_0$  from Ref. 15,

$$\gamma_0 = \frac{4\pi e^2 K^2 kT}{\varepsilon_s \hbar^2 V},$$

valid for the piezoelectric relaxation mechanism, as well as other parameters relevant to the present experiment, one concludes that in the hopping regime  $\sigma_2 \gtrsim \sigma_1$ . This conclusion agrees with the experimental results obtained for the middles of the Hall plateaus at 5.5 T and 2.7 T

and ensures that the conductance mechanism in these regions is indeed hopping.

Given an experimental value for  $\sigma_1$ , one can obtain from Eq. (9) the localization length  $\xi$  provided that the single-electron density of states,  $g$ , is known for given values of the magnetic field. This quantity has been obtained from the temperature dependence measurements of the thermally-activated dc conductivity.<sup>1,3</sup> It has been shown that for small filling factors the density of states in the plateau regions is finite and almost field-independent, see Fig. 8



FIG. 8. Schematic profile of the single-electron density of states

Using the density of states versus mobility curve from Ref. 1, obtained for a sample similar to ours, we estimate the density of states as  $g = 2.5 \times 10^{24} \text{ cm}^{-2} \cdot \text{erg}^{-1}$ . On the other hand, according to Ref. 3, the density of states as function of the magnetic field  $H$  can be expressed by the interpolation formula

$$g(H) = \frac{g_0}{1 + \sqrt{\mu H}}, \quad (11)$$

where  $\mu$  is the mobility of the 2D-electrons while  $g_0 = m/(\pi\hbar^2)$  is the 2D density of states at  $H = 0$ . From Eq. (11) we obtain for  $H = 5.5$  T the density of states  $g = 1.7 \times 10^{24} \text{ cm}^{-2} \cdot \text{erg}^{-1}$ .

Using the first estimate for the density of states one obtains  $\xi = 6.5 \times 10^{-6} \text{ cm}$ , that is about 1.6 times greater than the spacer thickness,  $l_{\text{sp}} = 4 \times 10^{-6} \text{ cm}$ . On the other hand, it is the spacer width which characterizes the random potential correlation length in the 2DEG layer. Hence, this fact contradicts our interpretation of experimental results in terms of pure nearest-neighbor pair hopping.

To solve the discrepancy, we assume that the high-frequency hopping conductivity of the 2DEG channel is shunted by hopping along the doping Si  $\delta$ -layer. This assumption can be substantiated as follows. Let us suppose that at the middle of the Hall plateau  $\sigma_1^{\nu=2} = 4 \times 10^{-7} \text{ Ohm}^{-1}$  and  $\sigma_2^{\nu=2} = 2.4 \times 10^{-6} \text{ Ohm}^{-1}$  are entirely determined by the hopping conductivity along the Si  $\delta$ -layer. Such a contribution is only weakly dependent on the magnetic field because the latter is too weak to deform significantly the wave functions of the Si-dopants. Then the contributions to  $\sigma_i$  associated with the 2DEG channel are just the difference between the experimentally measured  $\sigma_i$  in a given magnetic field and its value at  $\nu = 2$ .

We now analyze the dependence of the differences  $F_1 \equiv$

$\sigma_1 - \sigma_1^{\nu=2}$  and  $F_2 \equiv \sigma_2 - \sigma_2^{\nu=2}$  on the filling factor  $\nu$ . The plots of  $\lg F_i$  versus  $\nu$  are shown in Fig. 9. Both curves approach straight lines, and consequently can be extrapolated to  $\nu = 2$ . Using this extrapolation we have obtained  $F_1^{\nu=2} = 10^{-8} \text{ Ohm}^{-1}$  and  $F_2^{\nu=2} = 5 \times 10^{-8} \text{ Ohm}^{-1}$ . It should be noticed here that the extrapolated values of  $F_i^{\nu=2}$  are two orders of magnitude smaller than the values of  $\sigma_i^{\nu=2}$ , associated with the hopping along Si- $\delta$ -layer.

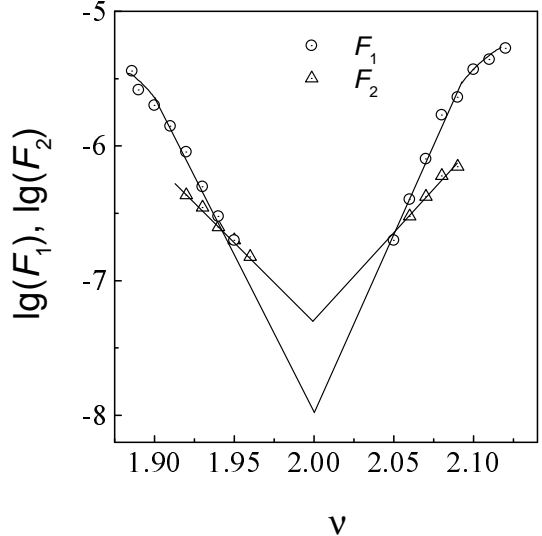


FIG. 9. The dependences of  $\lg(F_1) = \lg(\sigma_1 - \sigma_1^{\nu=2})$  and  $\lg(F_2) = \lg(\sigma_2 - \sigma_2^{\nu=2})$  versus the filling factor  $\nu$  near  $\nu = 2$ .  $T = 1.5 \text{ K}$ ,  $f = 30 \text{ MHz}$ .

Using the extrapolated values of  $F_1$  and  $F_2$  to extract the 2DEG contributions to  $\sigma_1$  and  $\sigma_2$ , one can calculate the electron localization length at  $\nu = 2$  from Eq. (9). This procedure is corroborated by the fact that the experimental ratio  $F_2/F_1 = 5$  is close to the theoretical value 4.2 coming from Eq. (10). The localization length at  $\nu = 2$  obtained in this way is  $\xi = 2 \times 10^{-6} \text{ cm}$ , which is half of the spacer width. This estimate makes realistic the "two-site model" which we have extensively used. It should be emphasized, however, that from the above value of  $\xi$  the hopping length  $r_\omega$  is estimated to be  $1.4 \times 10^{-5} \text{ cm}$ . Consequently, there is an interplay between hops to the nearest and more remote neighbors. A more rigorous theory for this situation should be worked out. Such a theory should also explain why the magnetic field dependences of  $\sigma_1$  and  $\sigma_2$  at the vicinity of  $\nu = 2$  appear to be different – the  $\sigma_1(H)$ -dependence is more pronounced than the  $\sigma_2(H)$ -one. According to the two-site model, both are determined by the respective dependence of the localization length on the magnetic field and should be similar. Indeed, their ratio, from Eq. (10), is almost field-independent. It follows from the experimental data that there exists an additional mechanism leading to the pronounced decrease of  $\sigma_2$  as the Fermi level falls into the extended states region. A probable mechanism is thermal activation of electrons from the Fermi level to the upper Landau band, leading, firstly,

to a decrease of the number of pairs responsible for the hopping conductivity, and, secondly to a screening of the electric field amplitude produced by the SAW. We hope to work out a proper quantitative theory in future.

#### IV. CONCLUSIONS

The above analysis leads to the following conclusions:

- At the vicinity of the Hall plateau centers, high-frequency hopping conductance in the 2DEG layer can be effectively shunted by hopping inside the doping  $\delta$ -layer.
- When the shunting effect is properly subtracted, the results appear to be compatible with the nearest neighbor two-site model of hopping conductivity.
- The localization length determined at different magnetic fields (and, consequently, different filling factors) by the above method scales as the magnetic length  $a_H = (\hbar/eH)^{1/2}$ . This agrees with the concept of nearest-neighbor hopping.
- The interpretation of the imaginary part of the conductivity,  $\sigma_2(\omega)$ , appears more complicated. While the magnetic field dependence of the real part of the hf hopping conductivity of 2D electrons seems to be determined by the magnetic field dependence of the localization length – the slope of  $\lg \xi(H)$ , calculated from the values of  $F_1^{\nu=2}(H)$  using Eq. (9), is close to the slope of  $\lg \xi(H)$  in Ref. 2 – the magnetic field dependence of the imaginary part of the hf conductivity has been explained so far only qualitatively. A more detailed quantitative analysis, which would include a proper account of the screening of the SAW-induced hf electrical field by both layers, is required.

It is worth emphasizing that the acoustic method used in the present work allows the determination of the localization length near the Hall plateau centers. This is very difficult to achieve using a dc technique.

#### V. ACKNOWLEDGMENTS

The work is supported by RFFI N 98-02-18280, MN-TFR N 97-1043 grants and I. L. Drichko was supported by the grant of Research Council of Norway. We are grateful to Ora Entin-Wohlman for reading the manuscript and useful remarks.

#### APPENDIX A: DERIVATION OF $\sigma(\omega)$

The derivations of the complex  $\sigma(\omega)$  within the two-site approximation have been extensively discussed, see

e. g. Refs. 14 and 15. However, the resulting formulae differ in some details. These differences are mainly due to different assumptions about the relaxation of the occupation numbers of the localized states. We therefore present here a unified derivation, in order to clarify the various assumptions and notations.

Let us characterize the sites by the single-electron energies  $\varphi_{1,2}$  which would be the actual energies if the Coulomb correlation between the occupation numbers is ignored. The two electron energies, in the absence of quantum hybridization of the states, can be specified by 4 terms,

$$W_0 = 0, \quad W_1 = \varphi_1, \quad W_2 = \varphi_2, \quad W_3 = \varphi_1 + \varphi_2 + \frac{e^2}{\varepsilon_s r}.$$

Here  $r$  is the distance between the sites. As shown in Ref. 14, when the frequency  $\omega$  and the temperature  $T$  are low enough, such that  $\hbar\omega, kT \ll e^2/\varepsilon_s r$  only the two terms  $W_1$  and  $W_2$  can be occupied, and we face a situation of a two-level electronic system (TLS). Quantum tunneling hybridizes the two levels, so that the resulting energies are

$$W_{\pm} = \frac{\varphi_1 + \varphi_2}{2} \pm \frac{E}{2}, \quad E = \sqrt{\Delta^2 + \Lambda^2(r)}.$$

Here  $\Delta = \varphi_1 - \varphi_2$ ,  $\Lambda(r)$  is the energy overlap integral which decays as  $r$  increases. The effective Hamiltonian corresponding to this situation is

$$\mathcal{H}_{LR} = \frac{1}{2} \begin{pmatrix} \Delta & -\Lambda \\ -\Lambda & -\Delta \end{pmatrix} = \frac{1}{2} (\Delta \sigma_z - \Lambda \sigma_x). \quad (A1)$$

Here  $\sigma_i$  are the Pauli matrices. Diagonalizing this Hamiltonian we obtain  $\mathcal{H}_0 = (E/2) \sigma_z$ .

The quantities  $\varphi_i$  are random, and their distributions are specified as follows.<sup>14</sup> The “center-of-gravity”,  $(\varphi_1 + \varphi_2)/2$  is assumed to be uniformly distributed within a band of width  $e^2/\varepsilon_s r$ ; and the difference,  $\Delta \equiv \varphi_1 - \varphi_2$ , is also assumed to be uniformly distributed within a band much wider than  $kT$ . Since  $d^2r = r dr d\phi$  where  $\phi$  is the polar angle in the 2DEG plane, we obtain an  $r$ -independent pair distribution function  $\mathcal{P}(\Delta, r, \phi) = g^2 e^2 / \varepsilon_s$  where  $g$  is the (constant) single-electron density of states. It is convenient to change the variables from  $\Delta, r, \phi$  to  $\Delta, \Lambda, \phi$ ,

$$\mathcal{P}(\Delta, \Lambda, \phi) = g^2 (e^2 / \varepsilon_s) |dr_\Lambda / d\Lambda|, \quad (A2)$$

where  $r_\Lambda$  is the solution of the equation  $\Lambda(r) = \Lambda$ .

In the presence of an external ac electric field  $\mathbf{E}$  the pair acquires a dipole moment  $\hat{\mathbf{d}} = e\hat{\mathbf{r}}$ , described by the interaction Hamiltonian  $\mathcal{H}_i = (\mathbf{E} \cdot \hat{\mathbf{d}}) = e(\mathbf{E} \cdot \hat{\mathbf{r}})$ . This interaction is added to  $\Delta$  in the Hamiltonian (A1). In the representation where  $\mathcal{H}_0$  is diagonal, the interaction Hamiltonian becomes

$$\mathcal{H}_{\text{int}} = e(\mathbf{E} \cdot \hat{\mathbf{r}}) \left( \frac{\Delta}{E} \sigma_z - \frac{\Lambda}{E} \sigma_x \right). \quad (\text{A3})$$

The contribution of a pair to the complex  $\sigma(\omega)$  can be expressed in terms of the complex susceptibility,  $\chi(\omega) = \sigma(\omega)/i\omega$  which in turn is given by (cf. Ref. 16)

$$\chi(\omega) = \frac{\pi e^4 g^2}{\varepsilon_s} \int d\Delta d\Lambda r_\Lambda^2 |dr_\Lambda/d\Lambda| \times \left[ (\Delta/E)^2 \chi_{zz}(\omega) + (\Lambda/E)^2 \chi_{xx}(\omega) \right]. \quad (\text{A4})$$

The partial susceptibilities  $\chi_{pq}$  are given by (cf. Ref. 16)

$$\chi_{zz} = \frac{1}{kT \cosh^2(E/2kT)} \frac{i\gamma_{\parallel}}{\omega + i\gamma_{\parallel}} \quad (\text{A5})$$

$$\chi_{xx} = \tanh\left(\frac{E}{2kT}\right) \sum_{\pm} \mp \frac{\hbar^{-1}}{\omega \mp E/\hbar + i\gamma}, \quad (\text{A6})$$

where  $\gamma$  and  $\gamma_{\parallel}$  are the proper relaxation rates.  $\chi_{zz}$  is responsible for the relaxational contribution, while  $\chi_{xx}$  is responsible for the resonant one.

To continue the calculations one needs to specify the spatial dependence of the overlap integral. Let us assume that  $\Lambda(r) = J e^{-r/\xi}$ , where  $\xi$  is the localization length. Then,  $r_\Lambda = \xi \ln(J/\Lambda)$ ,  $|dr_\Lambda/d\Lambda| = \xi/\Lambda$ . At the next step, it is convenient to transform the variables from  $\Delta, \Lambda$  to  $E, p = (\Lambda/E)^2$ , the Jacobian being  $(2p)^{-1}(1-p)^{-1/2}$ . This results in

$$\tilde{\chi}(\omega) \equiv \frac{\chi(\omega)}{\chi_0} = \int_0^\infty d\epsilon \int_0^1 \frac{dp}{p\sqrt{1-p}} \ln^2\left(\frac{\tilde{J}}{\epsilon\sqrt{p}}\right) \times [p\chi_{xx}(\omega) + (1-p)\chi_{zz}(\omega)] \quad (\text{A7})$$

where  $\chi_0 = \pi e^4 g^2 \xi^3 kT/2\varepsilon_s$ ,  $\epsilon = E/kT$ , and  $\tilde{J} = J/kT \gg 1$ .

The following analysis will be based on Eq. (A7). It can be easily shown that under the conditions of the present experiment the only important contribution to the dissipative part of the susceptibility,  $\text{Im } \tilde{\chi}(\omega)$ , is the one coming from the relaxational mechanism,  $\chi_{zz}$ . Thus we have,

$$\text{Im } \tilde{\chi}(\omega) = \int_0^\infty \frac{d\epsilon}{\cosh^2(\epsilon/2)} \int_0^1 \frac{dp \sqrt{1-p}}{p} \times \ln^2\left(\frac{\tilde{J}}{\epsilon\sqrt{p}}\right) \frac{\gamma_{\parallel}\omega}{\omega^2 + \gamma_{\parallel}^2}. \quad (\text{A8})$$

An important feature of the relaxation rate  $\gamma_{\parallel}$  is that  $\gamma_{\parallel}(\epsilon, p) = p\gamma_0(\epsilon)$ , see e. g. Ref. 15. Since we are interested in the case  $\omega \ll \gamma_0$ , we can put  $\epsilon = 1$ ,  $p = p_\omega \equiv \sqrt{\gamma_0(1)/\omega}$  in the argument of the logarithm and take the logarithm out of the integrand. As a result,

$$\text{Im } \tilde{\chi} = \pi \left( \mathcal{L}_T + \frac{1}{2} \mathcal{L}_\omega \right)^2, \quad (\text{A9})$$

where  $\mathcal{L}_T = \ln \tilde{J} \gg 1$  while  $\mathcal{L}_\omega = \ln(1/p_\omega) \gg 1$ .

The relaxational contribution to the real part can be written as

$$\begin{aligned} \text{Re } \tilde{\chi}_{zz}(\omega) &= \int_0^\infty \frac{d\epsilon}{\cosh^2(\epsilon/2)} \int_0^1 \frac{dp \sqrt{1-p}}{p} \ln^2\left(\frac{\tilde{J}}{\epsilon\sqrt{p}}\right) \\ &\times \frac{\gamma_{\parallel}^2}{\omega^2 + \gamma_{\parallel}^2} \approx 2 \int_{p_\omega}^1 \frac{dp}{p} \left( \mathcal{L}_T - \frac{1}{2} \ln p \right)^2 \\ &= 2\mathcal{L}_\omega \left( \mathcal{L}_T^2 + \frac{1}{2} \mathcal{L}_T \mathcal{L}_\omega + \frac{1}{12} \mathcal{L}_\omega^2 \right). \end{aligned} \quad (\text{A10})$$

The contribution from  $\chi_{xx}$  to the real part of the susceptibility is also important. Putting  $\hbar\omega \ll E$  we obtain

$$\begin{aligned} \text{Re } \tilde{\chi}_{xx} &= 2 \int_0^\infty \frac{d\epsilon}{\epsilon} \tanh(\epsilon/2) \int_0^1 \frac{dp}{\sqrt{1-p}} \ln^2\left(\frac{\tilde{J}}{\epsilon\sqrt{p}}\right) \\ &\approx 4\mathcal{L}_T^2 \int_0^\infty \frac{d\epsilon}{\epsilon} \tanh\left(\frac{\epsilon}{2}\right). \end{aligned} \quad (\text{A11})$$

The last integral diverges logarithmically at its upper limit. That means that the result is substantially dependent on the total structure of the impurity band. Assuming that (i)  $e^2/\varepsilon_s \xi \mathcal{L}_T \ll \hbar\omega_c$ , and (ii) that we are interested in the situation when the Fermi level is in the middle of the gap, we can replace for a *very crude* estimate

$$g^2 \int_0^\infty \frac{d\epsilon}{\epsilon} \tanh\left(\frac{\epsilon}{2}\right) \quad \text{by} \quad \int_0^\infty \frac{d\epsilon}{\epsilon} g^2(\epsilon) \tanh\left(\frac{\epsilon}{2}\right).$$

According to certain experimental evidence, the density of localized states within the gap is a weak function of the energy. Then an estimate for the above integral can be written as  $c g^2 \mathcal{L}_c$  where  $\mathcal{L}_c = \ln(\hbar\omega_c/kT)$ , while  $c \gtrsim 1$  is a correction factor due to energy dependence of the density of states. As a result, we obtain

$$\text{Re } \tilde{\chi}_{xx} \approx 4c \mathcal{L}_T^2 \mathcal{L}_c. \quad (\text{A12})$$

Since  $\text{Re } \sigma / \text{Im } \sigma = \text{Im } \chi / \text{Re } \chi$  we obtain Eq. (10).

---

<sup>1</sup> D. Weiss, K. v. Klitzing, and V. Mosser, in *Two Dimensional Systems: Physics and New Devices*, edited by G. Bauer, F. Kuchar and F. Heinrich (Springer-Verlag, Berlin, 1986).

<sup>2</sup> M. Furlan, Phys. Rev. B **57**, 14818 (1998).

<sup>3</sup> M. V. Gavrilov and I. V. Kukushkin, JETP Lett. **43**, 79 (1986).

<sup>4</sup> F. Tremblay, M. Pepper, R. Newbury, D. A. Ritchie, D. C. Peacock, J. E. F. Frost, G. A. C. Jones, and G. Hill, J. Phys.: Cond. Mat. **2**, 7367 (1990).

<sup>5</sup> F. W. VanKeuls, X. L. Xu, H. W. Jiang, and A. J. Dahm, Phys. Rev. B **56**, 1161 (1997).

<sup>6</sup> S. I. Khondaker, I. S. Shlimak, J. T. Nicholls, M. Pepper, and D. A. Ritchie. Proc. of the 24 Int. Conf. on the Physics of Semiconductor, (Jerusalem, Israel) ed. by D. Gershoni (World Scientific, 1998) on CD-ROM.

<sup>7</sup> I. L. Drichko, A. M. D'yakonov, I. Yu. Smirnov, V. V. Preobrazhenskii and A. I. Toropov, Semiconductors **33**, 892 (1999).

<sup>8</sup> V. D. Kagan, Semiconductors **31**, 470 (1997).

<sup>9</sup> I. L. Drichko and I. Yu. Smirnov, Semiconductors **31**, 933 (1997).

<sup>10</sup> A. Wixforth, J. P. Kotthaus, and G. Weimann, Phys. Rev. Lett. **56**, 2104 (1986); A. Schenstrom, Y. J. Quian, M. F. Xu, H. P. Baum, H. Levy, and B. K. Sarma, Sol. State Comm. **65**, 739 (1988).

<sup>11</sup> I. L. Drichko, A. M. D'yakonov, A. M. Kreshchuk, T. A. Polyanskaya, I. G. Savel'ev, I. Yu. Smirnov, and A. V. Suslov, Semiconductors **31**, 384 (1997).

<sup>12</sup> I. L. Drichko, A. M. D'yakonov, V. D. Kagan, I. Yu. Smirnov, and A. I. Toropov, Proc. of the 24 Int. Conf. on the Physics of Semiconductors (Jerusalem, Israel) ed. by D. Gershoni (World Scientific, 1998) on CD-ROM.

<sup>13</sup> A. L. Efros, Zh. Eksp. Teor. Fiz. **89**, 1834 (1985) [Sov. Phys. JETP **62**, 1057 (1985)].

<sup>14</sup> A. L. Efros and B. I. Shklovskii, In: *Electron-Electron Interactions in Disordered Systems*, ed. by A. L. Efros and M. Pollak, Elsevier, B. V. (1985), p. 409.

<sup>15</sup> Yu. M. Galperin, V. L. Gurevich, and D. A. Parshin, in *Hopping Transport in Solids*, ed. by B. Shklovskii and M. Pollak, Elsevier, 1991.

<sup>16</sup> S. V. Maleev, Zh. Eksp. Teor. Fiz. **84**, 260 (1983) [Sov. Phys. JETP **57**, 149 (1983)].